JOC Article

Cyclic Allene Intermediates in Intramolecular Dehydro Diels−Alder Reactions: Labeling and Theoretical Cycloaromatization Studies†

David Rodríguez, Armando Navarro-Vázquez, Luis Castedo, Domingo Domínguez,* and Carlos Saá*

Departamento de Química Orgánica y Unidad Asociada al CSIC, Facultad de Química, Universidad de Santiago de Compostela, 15782 Santiago de Compostela, Spain

qocsaa@usc.es

Received October 8, 2002

A comprehensive theoretical and experimental investigation of dehydro Diels−Alder reactions examining the evolution of the cyclic allene intermediates under conditions for intramolecular and ionic and radical intermolecular cycloaromatization processes is reported. Theoretical calculations showed that the most favored intramolecular path for cycloaromatization of 1,2,4-cyclohexatriene **4** and its benzoannulated derivative **14**, strained cyclic allenes, consists of a pair of successive [1,2] H shifts rather than a [1,5] shift. Cycloaromatization of cyclic allenes may follow both inter- and intramolecular pathways, depending on the experimental conditions (use of protic or aprotic solvents). For synthetic purposes, the best procedure is to use a protic solvent to promote the ionic intermolecular route, the fastest and highest yielding. When the reaction is carried out in CCl_4, intermolecular radical addition of chlorine to the cyclic allene competes with intramolecular aromatization paths. Theoretical calculations predict a low barrier for the reaction of cyclic allenes with carbon tetrachloride, and that the cyclic allenes act as nucleophiles in this reaction.

Introduction

The intramolecular dehydro Diels−Alder reactions (intramolecular [4+2] cycloadditions) of alkynes with certain enynes have long been known[1] and are well-documented.[2] During the past decade considerable effort has gone into generalizing this cyclization to other enynes[3] and arylacetylenes (arenynes)[4] so as to harness it for the synthesis of polycyclic aromatic compounds. For example, the intramolecular [4+2] cycloadditions of **1a**−**d** give the tetracyclic nuclei of benzo[*b*]fluorenes **2a**−**d**[5] and benzo[*a*]fluorene **3d**,[6] which belong to classes of natural compounds that exhibit interesting biological activity (Scheme 1).[7]

The intermediates in these reactions are 1,2,4-cyclohexatrienes, strained cyclic allenes[8] that are also observed in the electrocyclization of 1,3-hexadien-5-ynes[9] and which normally evolve to aromatic products by isomerization. For the reaction of diarylacetylenes **1**[5b,c] in the presence of MeOH(D) as proton source, deuterium experiments have recently demonstrated that this isomerization takes place by means of an intermolecular ionic mechanism rather than an intramolecular hydrogen shift (Scheme 2).[10]

These experimental results can be explained in terms of the bonding in the putative intermediates. Specifically, we have shown that the allene moiety of cyclic allenes

† This paper is dedicated to the late Prof. Antonio González González.

(1) Michael, A.; Bucher, J. E. *Chem. Ber.* **1895**, *28*, 2511−2512.

(2) (a) Dykstra, H. B. *J. Am. Chem. Soc.* **1934**, *56*, 1625−1628. (b) Butz, L. W.; Joshel, L. M. *J. Org. Chem.* **1941**, *6*, 3344. Butz, L. W.; Joshel, L. M. *J. Org. Chem.* **1942**, *7*, 1311. (c) Baddar, F. G.; El-Assal, L. S.; Doss, N. A. *J. Chem. Soc.* **1959**, 1027−1032. (d) Brown, D.; Stevenson, R. *J. Org. Chem.* **1965**, *30*, 1759−1763. (e) Klemm, L. H.; Gopinath, K. W.; Lee, D. H.; Kelley, F. W.; Trod, E.; McGuire, T. M. *Tetrahedron* **1966**, *22*, 1797−1808. (f) Whitlock, H. W., Jr.; Wu, E.-M.; Whitlock, B. J. *J. Org. Chem.* **1969**, *34*, 1857−1859. (g) Bossenbroek, B.; Sanders, D. C.; Curry, H. M.; Shechter, H. *J. Org. Chem.* **1969**, *34*, 371−378.

(3) (a) Danheiser, R. L.; Gould, A. E.; Fernández de la Pradilla, R.; Helgason, A. L. *J. Org. Chem.* **1994**, *59*, 5514−5515. (b) Burrell, R. C.; Daoust, K. J.; Bradley, A. Z.; DiRico, K. J.; Johnson, R. P. *J. Am. Chem. Soc.* **1996**, *118*, 4218−4219. (c) González, J. J.; Francesch, A.; Cárdenas, D. J.; Echavarren, A. M. *J. Org. Chem.* **1998**, *63*, 2854−2857.

(4) Eckert, T.; Ipaktschi, J. *Monatsh. Chem.* **1998**, *129*, 1035−1048.

(5) (a) Schmittel, M.; Strittmatter, M.; Schenk, W. A.; Hagel, M. *Z. Naturforscher* **1998**, *53b*, 1015−1020. (b) Rodríguez, D.; Navarro, A.; Castedo, L.; Domínguez, D.; Saá, C. *Org. Lett.* **2000**, *2*, 1497−1500. (c) Rodríguez, D.; Castedo, L.; Domínguez, D.; Saá, C. *Tetrahedron Lett.* **1999**, *40*, 7701−7704. For synthesis of benzo[*b*]fluorenes by intramolecular [4+2] cycloaddition of alkynes to allenes, see: Frutos, O.; Echavarren, A. M. *Tetrahedron Lett.* **1997**, *38*, 7941−7942.

(6) Atienza, C.; Mateo, C.; de Frutos, O.; Echavarren, A. M. *Org. Lett.* **2001**, *3*, 153−155.

(7) (a) Gould, S. J. *Chem. Rev.* **1997**, *97*, 2499−2510. (b) Gould, S. J.; Melville, C. R.; Cone, M. C.; Chen, J.; Carney, J. R. *J. Org. Chem.* **1997**, *62*, 320−324. (c) Protean, P. J.; Li, Y.; Chen, J.; Thomas Williamson, R.; Gould, S. J.; Laufer, R. S.; Dmitrienko, G. I. *J. Am. Chem. Soc.* **2000**, *122*, 8325−8326 and references therein.

(8) For a review of the reactivity and structure of cyclic allenes, see: Johnson, R. P. *Chem. Rev.* **1989**, *89*, 1111−1124.

(9) (a) Roth, W. R.; Hopf, H.; Horn, C. *Chem. Ber.* **1994**, *127*, 1765−1779. (b) Hopf, H.; Berger, H.; Zimmermann, G.; Nüchter, U.; Jones, P. G.; Dix, I. *Angew. Chem., Int. Ed. Engl.* **1997**, *36*, 1187−1190. (c) Fernández-Zertuche, M.; Hernández-Lamoneda, R.; Ramírez-Solís, A. J. *J. Org. Chem.* **2000**, *65*, 5207−5211. (d) Prall, M.; Krüger, A.; Schreiner, P. R.; Hopf, H. *Chem. Eur. J.* **2001**, *7*, 4386-4394.

(10) Keto−enol isomerization of 3-hydroxy-1,2,4-cyclohexatriene to cyclohexa-2,5-dien-1-one through intramolecular proton transfer has recently been studied at the MP2(fc)/6-31G** level. The computed barrier to this process was only 6.7 kcal/mol, which suggests that the trapping of hydrogens in cyclic allenes made available by protic solvents may be a fast reaction. See ref 9c.

10.1021/jo0265380 CCC: $25.00
Published on Web 02/07/2003

SCHEME 1

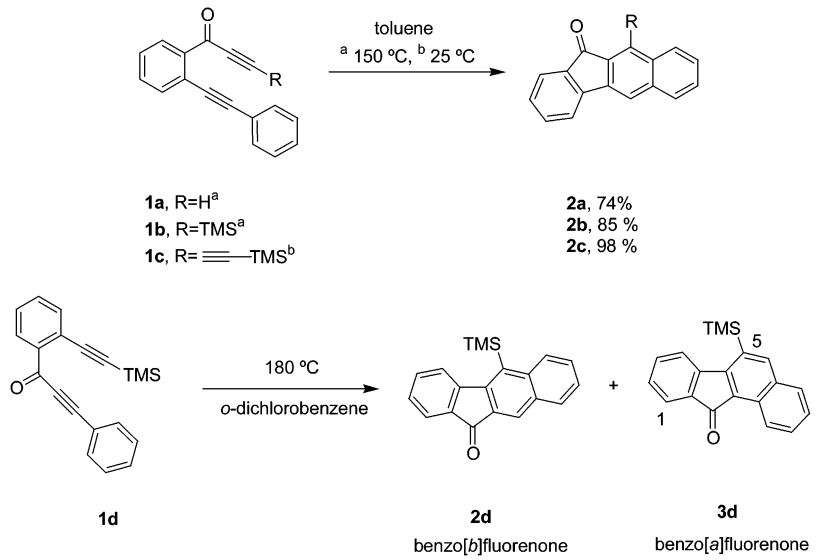

SCHEME 2

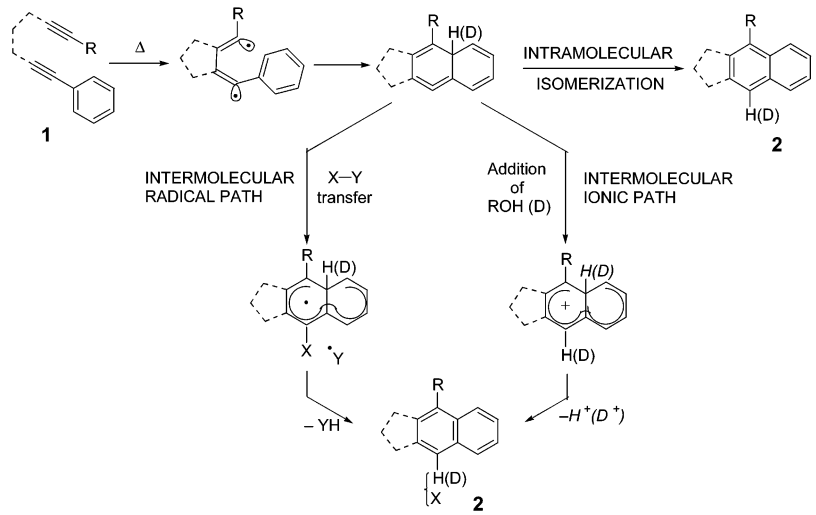

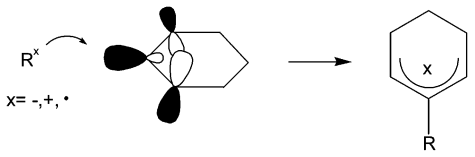

FIGURE 1. Reactivity of cyclic allenes.

can be regarded as featuring a bond between an sp^2-like orbital on the central carbon and an allyl π orbital (Figure 1),[5b] which allows the products and transition states of both intermolecular ionic and intermolecular radical reactions to benefit from allylic stabilization. This bonding may make the thermally allowed [1,5] hydrogen shift, sometimes postulated as an intramolecular pathway, significantly different from standard [1,5] H shifts.[11] To fully understand the intramolecular and ionic and radical intermolecular cycloaromatization processes of cyclic allenes we have undertaken a comprehensive investigation of the dehydro Diels–Alder reaction.

In the course of this work Hopf/Schreiner[12] have reported an excellent computational study about isomerization of 1,2,4-cyclohexatriene to benzene at BLYP and coupled-cluster BCCD(T) levels. They conclude that the most favored intramolecular path consists of a pair of successive [1,2] H shifts rather than a [1,5] shift.

Here we present the results of a comparable DFT/B3LYP computational study corroborating previous conclusions and the results of isotopic labeling experiments on the relative importance of intra- and intermolecular paths under protic, aprotic, and radical-generating conditions.

Computational Methodology

All structures were optimized by DFT methods, using the B3LYP[13,14] functional as implemented in Gaussian 98[15] in conjunction with the 6-31G*[16] basis set. Whether stationary

(11) For computational studies of the [1,5] H shift, see: Jiao, H.; Schleyer, P. v. R. *J. Chem. Soc., Faraday Trans.* **1994**, *90*, 1559–1567.

(12) (a) See ref 9d, see also comments in ref 56 of this work. (b) For several post-HF calculations, see: Anakinov, V. P. *J. Phys. Org. Chem.* **2001**, *14*, 109–121.

(13) Becke, A. D. *J. Chem. Phys.* **1993**, *98*, 5648–5652.

(14) Lee, C.; Yang, W.; Parr, R. G. *Phys. Rev. B* **1988**, 37, 785–789.

TABLE 1. Relative Energies (ΔH^{0K}, kcal/mol) of the Species Potentially Involved in Isomerization of Cyclohexatriene (4) and Isonaphthalene (14) at the B3LYP and CCSD(T) Levels

	4 (^{1}A)	**4i** (^{1}A)	**4ii** (^{3}A)	**5**	**6**	**7i** (^{1}A)	**7ii**(^{3}A)	**8**	**9**	**13**	**14**	**15**	**16**
B3LYP	0.0	2.2	4.6	49.6	27.8	5.8	2.2	11.2	61.6	−81.4	0.0	17.9	−101.5
CCSD(T)				48.0	31.9					−75.5	0.0	23.9	−91.7

points were minima or first-order saddle points was determined by analytical computation of vibrational frequencies. The minima connected via the saddle points detected were identified by visualization of the normal mode associated with the imaginary frequency. Zero-point vibrational energies were scaled by a factor of 0.9804.[17]

For high and low open-shell species an unrestricted formalism was used in the DFT calculations. When a restricted solution was obtained for species that include some biradical character, the stability of the determinant was confirmed by using the algorithm implemented in Gaussian 98.[18] In recent studies [9d,19,20] it has been proven that the use of the hybrid B3LYP functional in combination with unrestricted determinant can provide good activation and reaction energies in processes involving open-shell singlets, with a low computational cost.

For structures of closed-shell nature, further single-point calculations were performed at the CCSD(T)[21] level (single-reference coupled clusters methods are unreliable for molecules with strong biradical character; this is alleviated in ref 9d by the use of BCCD(T)[22] method). All coupled-cluster calculations used an RHF determinant as reference. For species **7**, further multireference calculations were performed at the MCQDPT2[23] level, using the PC-GAMESS[24] version of the GAMESS-US[25] package. All these coupled-cluster and multireference calculations used a cc-pVDZ basis set[26] and the frozen core approximation. Nucleus-Independent Chemical Shifts (NICS)[27] were determined by computation of the isotropic shielding tensors at the B3LYP/6-311+G**/B3LYP/6-31G* level, using the GIAO[28] method.

For intermolecular reactions with carbon tetrachloride, energies were computed by single-point calculations at the B3LYP/6-311+G**[16] level to minimize the impact of basis set superposition error. The role of the solvent was taken into account by single-point B3LYP/6-311+G** calculations on the B3LYP/6-31G* structures, using the Polarized Continuum model (PCM)[29] of Tomasi and co-workers.

Charges and Wiberg[30] bond indices were calculated by NBO[31] analysis of the B3LYP density.

Results and Discussion

Intramolecular Isomerization: Computational Studies. The structure of 1,2,4-cyclohexatriene has previously been computed at semiempirical,[32] DFT,[9d,19a,33] MP2,[12b] and MRCI[34] levels. These studies predict the chiral singlet ground-state structure **4**.[35] The reaction is highly exothermic, the reaction enthalpy ΔH^{0K} being −81.4 kcal/mol at the B3LYP level and −75.5 kcal/mol by CCSD(T) (Table 1).[36]

The [1,5] hydrogen shift path from **4** to **13** passes through the transition structure **5** (Scheme 3, path *a*), in which the reactive termini are brought together by a highly distorted geometry with a C6−C1−C2 bond angle of 94° (Figure 2). This transition structure shows some degree of asynchrony, as the C2−H distance, 1.377 Å, is appreciably shorter than C6−H (1.469 Å). Since C1 lies far from the plane defined by the other carbons, there is no aromatic stabilization and the barrier is very high, 49.6 kcal/mol at the B3LYP/6-31G* level and 48.0 kcal/mol by CCSD(T) calculations,[37] making it unlikely that this is the path followed in cyclohexatriene aromatization.

The alternative aromatization pathway *b* involves two [1,2] hydrogen shifts (Scheme 3). The first leads to the cyclohexa-2,4-dienylidene $\sigma-\pi$ diradical **7** via transition

(15) Frisch, M. J.; Trucks, G. W.; Schlegel, H. B.; Scuseria, G. E.; Robb, M. A.; Cheeseman, J. R.; Zakrzewski, V. G.; Montgomery, J. A., Jr.; Stratmann, R. E.; Burant, J. C.; Dapprich, S.; Millam, J. M.; Daniels, A. D.; Kudin, K. N.; Strain, M. C.; Farkas, O.; Tomasi, J.; Barone, V.; Cossi, M.; Cammi, R.; Mennucci, B.; Pomelli, C.; Adamo, C.; Clifford, S.; Ochterski, J.; Petersson, G. A.; Ayala, P. Y.; Cui, Q.; Morokuma, K.; Malick, D. K.; Rabuck, A. D.; Raghavachari, K.; Foresman, J. B.; Cioslowski, J.; Ortiz, J. V.; Baboul, A. G.; Stefanov, B. B.; Liu, G.; Liashenko, A.; Piskorz, P.; Komaromi, I.; Gomperts, R.; Martin, R. L.; Fox, D. J.; Keith, T.; Al-Laham, M. A.; Peng, C. Y.; Nanayakkara, A.; Gonzalez, C.; Challacombe, M.; Gill, P. M. W.; Johnson, B.; Chen, W.; Wong, M. W.; Andres, J. L.; González, C.; Head-Gordon, M.; Replogle, E. S.; Pople, J. A. *Gaussian 98*, Revision A.7; Gaussian, Inc.: Pittsburgh, PA, 1998.

(16) Hehre, W.; Radom, L.; Schleyer, P. v. R.; Pople, J. A. *Ab Initio Molecular Orbital Theory*; Wiley: New York, 1986.

(17) Wong, M. W. *Chem. Phys. Lett.* **1996**, *256*, 391−399.

(18) Bauernschmitt, R.; Ahlrichs, R. *J. Chem. Phys.* **1996,** *104*, 9047−9052.

(19) (a) Bettinger, H. F.; Schreiner, P. R.; Schaefer, H. F., III; Schleyer, P. v. R. *J. Am. Chem. Soc.* **1998**, *120*, 5741−5744. (b) Schreiner, P. R.; Prall, M. *J. Am. Chem. Soc.* **1999**, *121*, 8615−8617.

(20) For a clear treatment of this problem see: Gräfenstein, J.; Hjerpe, A. M.; Kraka, E.; Cremer, D. *J. Phys. Chem. A* **2000**, *104*, 1748−1761.

(21) Pople, J. A.; Head-Gordon, M.; Raghavachari, K. *J. Chem. Phys.* **1987**, *87*, 5968−5975.

(22) Handy, N. C.; Pople, J. A.; Head-Gordon, M.; Raghavachari, K.; Trucks, G. W. *Chem. Phys. Lett.* **1989**, *164*, 185.

(23) (a) Nakano, H. *J. Chem. Phys.* **1993**, *99*, 7983. (b) Nakano, H. *Chem. Phys. Lett.* **1993**, *207*, 372−378.

(24) Granovsky, A. A. www http://classic.chem.msu.su/gran/gamess/index.html.

(25) Schmidt, M. W.; Baldridge, K. K.; Boatz, J. A.; Elbert, S. T.; Gordon, M. S.; Jensen, J. H.; Koseki, S.; Matsunaga, N.; Nguyen, K. A.; Su, S. J.; Windus, T. L.; Dupuis, M.; Montgomery, J. A. *J. Comput. Chem.* **1993**, *14*, 1347.

(26) Davidson, E. R. *Chem. Phys. Lett.* **1996**, *260*, 514−517. For CC calculations orbitals were expressed as spherical harmonics whereas a Cartesian expression was used in MCQDTP2 calculations.

(27) Schleyer, P. v. R.; Maerker, C.; Dransfeld, A.; Jiao, H.; Hommes, N. J. R. v. E. *J. Am. Chem. Soc.* **1996**, *118*, 6317−6318.

(28) Wolinski, K.; Hilton, J. F.; Pulay, P. *J. Am. Chem. Soc.* **1990**, *112*, 8251−8260.

(29) Miertus, S.; Scrocco, E.; Tomasi *Chem. Phys.* **1981**, *55*, 117−129.

(30) Wiberg, K. *Tetrahedron* **1968**, *24*, 1083−1096.

(31) Reed, A. E.; Curtiss, L. A.; Weinhold, F. *Chem. Rev.* **1988,** *88*, 899−926.

(32) Janoschek, R. *Angew. Chem., Int. Ed. Engl.* **1992**, *31*, 476−478. These were MCSCF calculations with two electrons in two orbitals.

(33) Freeman, P. K.; Pugh, J. K. *J. Org. Chem.* **1999**, *64*, 3947−3953.

(34) Engels, B.; Schoneboom, J. C.; Munster, H. F.; Groetsch, S.; Christl, M. *J. Am. Chem. Soc.* **2002**, *124*, 287−297.

(35) Structure **4** undergoes racemization through the C_s singlet diradical transition structure **4i**, which we have computed to be 2.2 kcal/mol above **4** (the triplet C_s structure **4ii** is a minimum in the triplet surface and lies 4.6 kcal/mol above **4**). This value is very close to the AM1 value obtained by Janoschek[32] (2.0 kcal/mol) and also quite close to the BLYP value obtained by Schreiner (5.9 kcal/mol). All these values suggest that racemization of **4** is a very fast process (Scheme 3). However, post-HF methods such as BCCD(T) (ref 9d) and CASPT2 and MRCI (ref 34) indicate a higher value of about 10 kcal/mol.

(36) The apparent discrepancy between experimental and theoretical reaction enthalpies has recently been resolved; see ref 34.

(37) The QCISD(T)/6-311G** barriers to [1,5] H shifts in 1,3-cyclopentadiene and 1,3-pentadiene at 0 K are 29.7 and 40.0 kcal/mol, respectively. See ref 12.

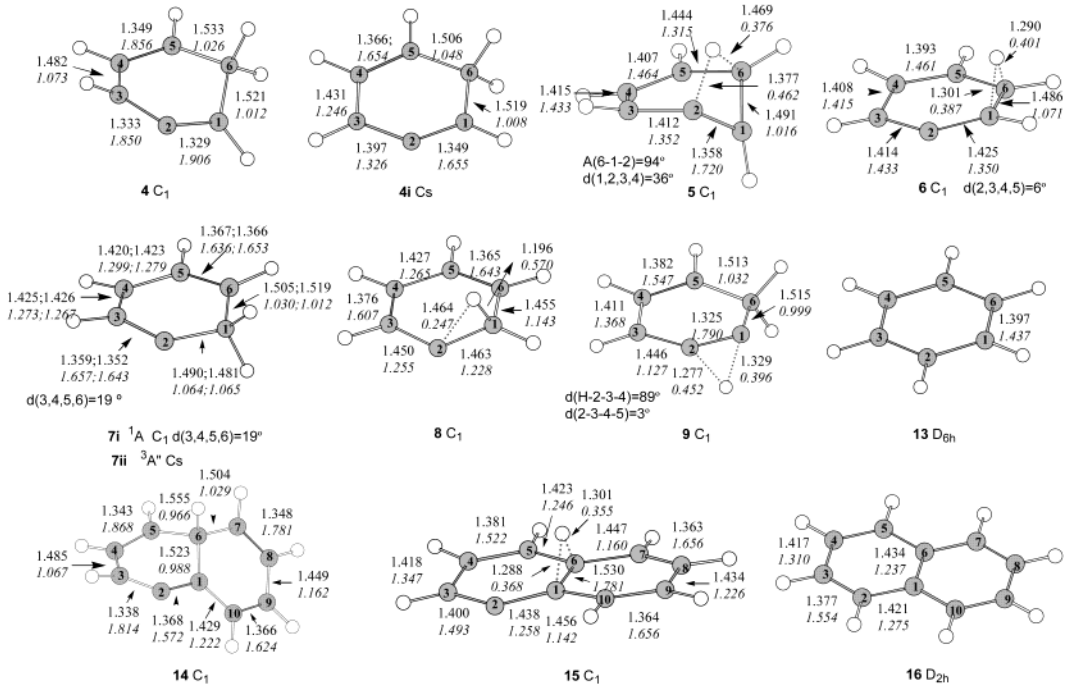

FIGURE 2. Geometrical parameters and bond orders (italics) of all computed species. For **7**, values for the singlet state **7i** are followed by values for the triplet state **7ii**.

SCHEME 3. Reaction Pathways for Intramolecular Isomerization of 1,2,4-Cyclohexatriene 4 to Benzene

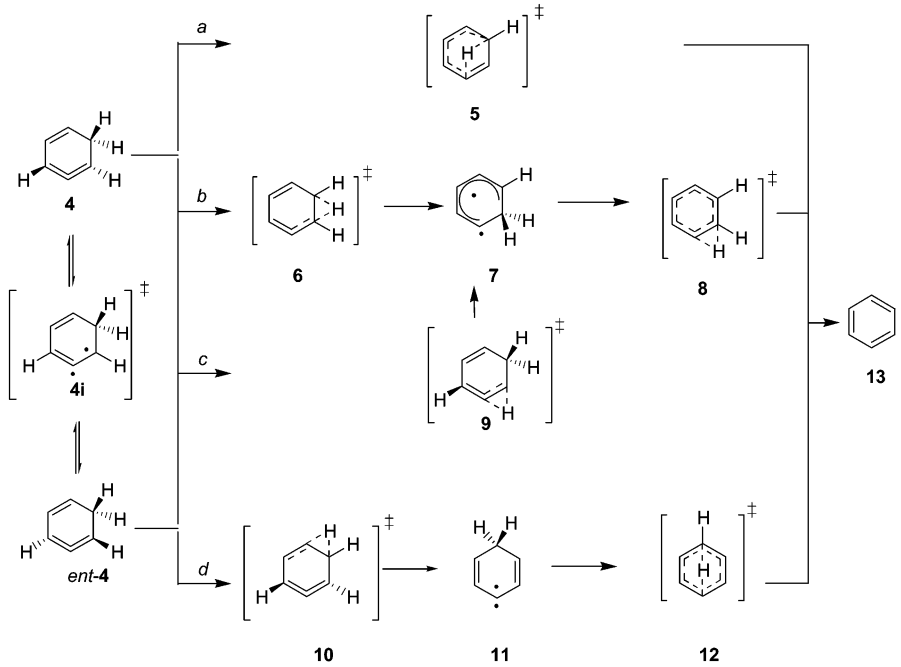

structure **6**. Schleyer and co-workers,[19,38] who studied this species at the B3LYP/TZ2P//B3LYP/DZP level as a possible intermediate in the topoisomerization of benzene, concluded that, unlike the C_s structure between **4** and *ent*-**4**, it has as a triplet ground-state structure; Hopf/Schreiner's[9d] BLYP calculations afforded a biradical singlet ground state (albeit with a very small singlet–triplet gap); and single-configuration BCCD(T) calculations predicted a zwitterionic structure. According to our B3LYP calculations the triplet state **7ii** is located 2.2 kcal/mol above **4** and 3.6 kcal/mol below the singlet state **7i**, a triplet–singlet gap even larger than that obtained by Schleyer, 2.9 kcal/mol; the preference for the triplet state at this computational level appears to be due to its strong delocalization of the π system endowing C2 with both σ and π spin density (Scheme 4) and thereby reducing electronic repulsion relative to the singlet state **7i**, in which C2 only has σ density. Multireference MCQDPT2(6,6) calculations on the geometry of **7ii** nevertheless afforded a singlet ground state lying 3.9 kcal/mol below the triplet state (and 31.9 kcal/mol below the most stable zwitterionic state), implying that, as

SCHEME 4. Resonant Structures and Spin Density Representation of Diradical 7 (^{3}A State)

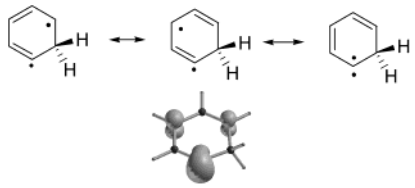

SCHEME 5

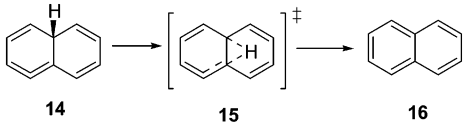

Hopf/Schreiner found, the true intermediate structure must also be in a singlet state. Note that the C3−C4−C5−C6 angle of 19° in the C_1 B3LYP singlet structure **7i** suggests a degree of $\sigma-\pi$ coupling. In both **7i** and **7ii** the C2−C3 and C5−C6 bonds are shorter than C3−C4 and C4−C5 because the former have double-bond character in two resonant structures and the latter in only one.

In the singlet surface the transition structure **6** presents a barrier of 27.8 kcal/mol to the process **4** → **7**. This is much lower than that for the [1,5] H shift. In **6**, the carbon skeleton is nearly planar (the C2−C3−C4−C5 dihedral angle is only 6°), which allows more efficient π overlapping than in **5**.

The second [1,2] hydrogen shift in path *b*, **7** → **8** → **13**, involves overcoming a barrier of only 5.4 kcal/mol from singlet **7i**. Transition structure **8**, in which the migrating hydrogen lies over the C1−C2 bond, is stabilized by conjugation beginning to extend to the sixth carbon atom. In keeping with this the geometry of **8** indicates an early transition, having C1−H and C2−H bond lengths of 1.196 and 1.464 Å, respectively.

Another possible path from **4** to singlet **7i** consists of a [1,2] hydrogen shift between C1 and C2 via transition structure **9** (path *c*, Scheme 3). However, this process involves overcoming a barrier of 62.8 kcal/mol. Due to the late attainment of the transition structure it has a strong biradical character, so much so that the unrestricted Kohn−Sham determinant fails to exhibit spatial spin-symmetry ($\langle S^2\rangle = 0.863$).

Hopf/Schreiner[9d] considered a fourth mechanism (path *d*, Scheme 3) in which the 1,1-biradical **11** is formed via the transition structure **10** (33 kcal/mol above **4**) and yields benzene **13** upon [1,4] hydrogen migration via transition structure **12**. However, the barrier to this second step is 48 kcal/mol, which clearly rules out this reaction path.

Effect of Benzoannulation. Benzo[*f*]annulation[39] of **4** to isonaphthalene **14** lowers the barrier to the first [1,2] hydrogen shift of path *b* (Scheme 5) by nearly 10 kcal/mol ($\Delta H = 17.9$ kcal/mol; see Table 1). This difference in activation enthalpy must be attributed to conjugation in transition state **15** being more extensive than in **6**, and

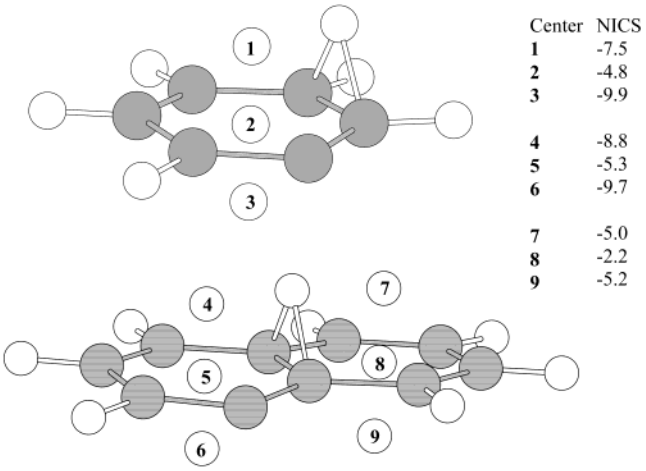

FIGURE 3. NICS at selected points in the vicinity of transition structures **6** and **15**.

means that intramolecular isomerization might well compete with intermolecular ionic or radical processes in the naphthalenic systems we have studied experimentally (Scheme 2).

All attempts to optimize a naphthalenic biradical analogue of **7** led to naphthalene (**16**), the biradical proving to be an inflection point rather than a minimum of the potential surface. The whole isomerization process **14** → **16** has an enthalpy of −101.5 kcal/mol. As in the parent system, the transition state **15** possesses a closed-shell character and a nearly planar geometry. Ten electrons contribute to the π system, and two occupy an sp^2-like orbital, centered on C2, lying in the molecular plane. The aromatic character of **15** is corroborated, as in **6**, by the bond lengths being more uniform than in the starting structure; the fact that C1−C6 is shortened to 1.486 Å in **6**, but elongated to 1.530 Å in **15**, is in keeping with their numbers of ring delocalized electrons, six and ten, respectively. The aromatic character is also indicated by the moderately negative NICS[27] calculated for the ring centers and for points 1.0 Å above and beneath them (see Figure 3).[40] At the same level, NICS of −8.0 and −10.2 ppm were obtained for points 0.0 and 1.0 Å above the center of the benzene molecule, and values of −8.6 and −10.6 ppm for the naphthalene molecule.

Summing up, as Hopf/Schreiner found,[9d] the [1,5] hydrogen shift ought not to be an operative pathway for the isomerization of 1,2,4-cyclohexatriene to benzene, which may, however, take place through a path of much lower energy consisting of two consecutive [1,2] hydrogen shifts, the rate-limiting first shift leading to cyclohexa-2,4-ylidene as intermediate. Benzoannulation significantly favors this intramolecular pathway due to extension of the conjugation system of the first transition structure.

Experimental Results: Isotopic Labeling. To compare the intermolecular ionic path with the intramolecular path we studied the thermal behavior of deuterated ynone **1a**-d_5 in the presence and absence of a proton source. Compound **1a**-d_5 was prepared following the

(38) The transition structures **6** and **8** were also computed in ref 19, with geometric results very close to ours.

(39) Hopf/Schreiner found that benzo[*c*]annulation of cyclohexatriene increased the barrier to aromatization via path *b*; see ref 9d.

(40) Calculations for this set of points minimizes the effects of σ bonds on NICS.

SCHEME 6

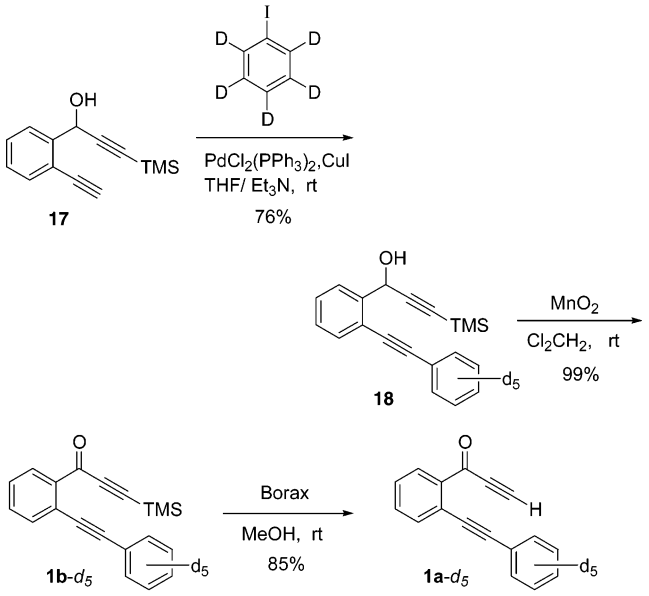

SCHEME 7

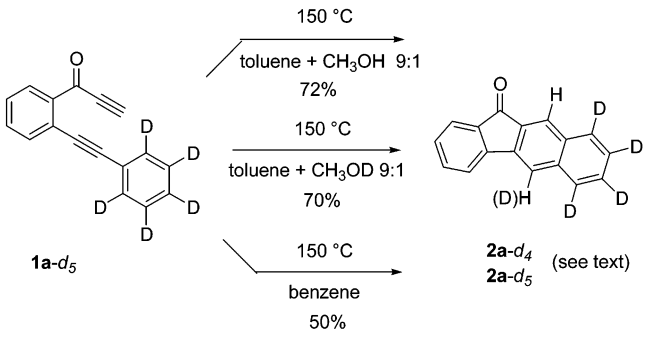

sequence depicted in Scheme 6: Sonogashira coupling of arylacetylene **17**[41] with iodobenzene-d_5 gave a 76% yield of the diarylacetylenic alcohol **18**, which quantitative oxidation to ketone **1b**-d_5 and subsequent desilylation with Borax[42] transformed into the desired deuterated ynone **1a**-d_5 in 85% yield.

Heating a solution of **1a**-d_5 in 90:10 (v/v) toluene/MeOH for 10 h in a sealed tube at 150 °C gave benzo[*b*]fluorenone **2a**-d_4 in 72% yield with no accompanying **2a**-d_5 (Scheme 7); similarly, when a 90:10 mixture of toluene/MeOD was used, benzo[*b*]fluorenone **2a**-d_5 was obtained with no **2a**-d_4. Heating a dry, deoxygenated 25 mM solution of **1a**-d_5 in benzene for 10 h in a sealed tube at 150 °C gave a 50% yield of benzo[*b*]fluorenone **2a**, 60% as **2a**-d_5 and 40% as **2a**-d_4 (Scheme 7).[43] The appearance of **2a**-d_4 is attributed to an ionic intermolecular path involving adventitious proton sources.

Due to a certain instability of ynone **1a**-d_5, we decided also to evaluate the thermal behavior of the stable silylated ynone **1b**-d_5 (Scheme 8). Surprisingly, heating a benzene solution of **1b**-d_5 for 10 h in a sealed tube at

SCHEME 8

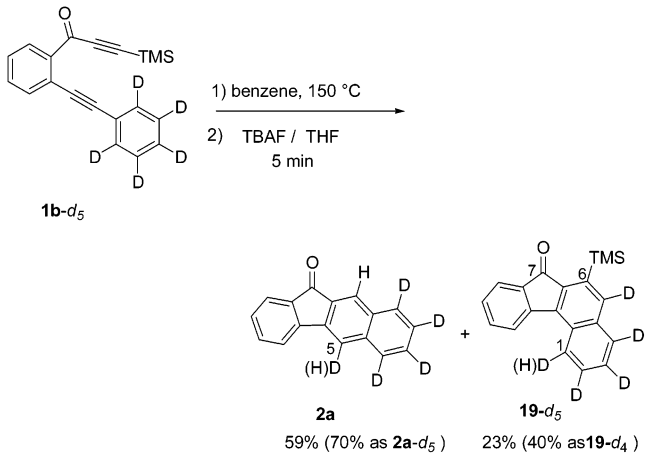

150 °C afforded two silylated products with similar TLC retention factors. Treatment of a THF solution of the reaction mixture with TBAF for 5 min allowed separation of a 59% yield of the expected desilylated benzo[*b*]fluorenone **2a** (70% as **2a**-d_5) from a 23% yield of the rearranged silylated benzo[*c*]fluorenone **19**[44] (60% as **19**-d_5, 40% as **19**-d_4). It is worth noting that **19**, unlike **2b**, failed to desilylate under mild conditions.[45]

Rearranged aromatic products like those from dehydro Diels–Alder reactions such as **19** have also been obtained from other TMS-ethynyl-substituted starting compounds.[6,46] In the present case, rearrangement will have involved production of the 1,2-dehydro[10]annulene **21a** by opening of the initial cyclic allene intermediate **20**, isomerization of **21a** to **21b**, [1,6]-electrocyclization of **21b** to a second cyclic allene **22**, and aromatization of the latter to the rearranged benzo[*c*]fluorenone **19** (Scheme 9).

Finally, we compared the intermolecular radical path with the intramolecular path by studying the thermal behavior of ynone **1b** in CCl_4.[47] Heating a 127 mM CCl_4 solution of **1b** for 10 h in a sealed tube at 150 °C afforded both a fraction containing products of the intramolecular path (a 6.5:1 mixture of benzo[*b*]- and benzo[*c*]fluorenones **2b** and **19**[44] in 41% combined yield) and a fraction containing a 32% yield of the product of the intermolecular path, the 5-chlorobenzo[*b*]fluorenone **23** (Scheme 10). Remarkably, not only did the two cycloaromatization pathways compete, but the ratio of the linear to the rearranged product of the intramolecular path, 6.5:1, was higher than under nonradical conditions (2.5:1, Scheme 8).

(41) Brückner, R. *Synlett* **1994**, 51–53. Brückner, R. *Liebigs Ann.* **1996**, *C41*, 447–456 and 457–471.

(42) Walton, D. R. M.; Waugh, F. *J. Organomet. Chem.* **1972**, *37*, 45–56.

(43) Determined by integration of the signals of the ^{1}H NMR of the purified product.

(44) Thermolysis of **1b** followed by desilylation gave a 61% yield of **2a** and 28% yield of **19** (nondeuterated), this latter confirmed by X-ray analysis. Rodríguez, D.; Navarro-Vázquez, A.; Castedo, L.; Domínguez, D.; Saá, C. *Tetrahedron Lett.* **2002**, *43*, 2717–2720.

(45) Toyota, M.; Terashima, S. *Tetrahedron Lett.* **1989**, *30*, 829–832.

(46) Rodríguez, D.; Navarro-Vázquez, A.; Castedo, L.; Domínguez, D.; Saá, C. *J. Am. Chem. Soc.* **2001**, *123*, 9178–9179.

(47) A pending question is whether the conversion of a cyclic allene to an aromatic ring might be bimolecular rather than unimolecular even in the absence of proton sources other than the cyclic allene itself, the proton at position 5 of **2a**, for example, being provided by a second molecule of the substrate. Unfortunately, no clear answer to this question was provided by the MS spectrum of the products of the crossover experiment we carried out to investigate this (heating a 1:5 mixture of **1b** and **1b**-d_5 in benzene, followed by treatment with TBAF).

SCHEME 9

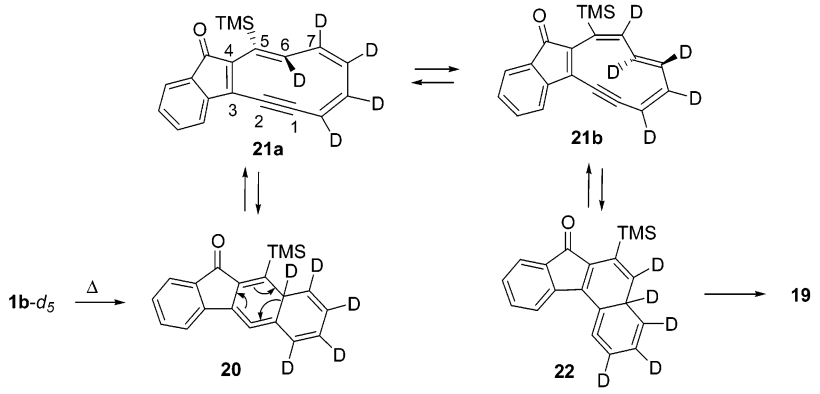

SCHEME 10

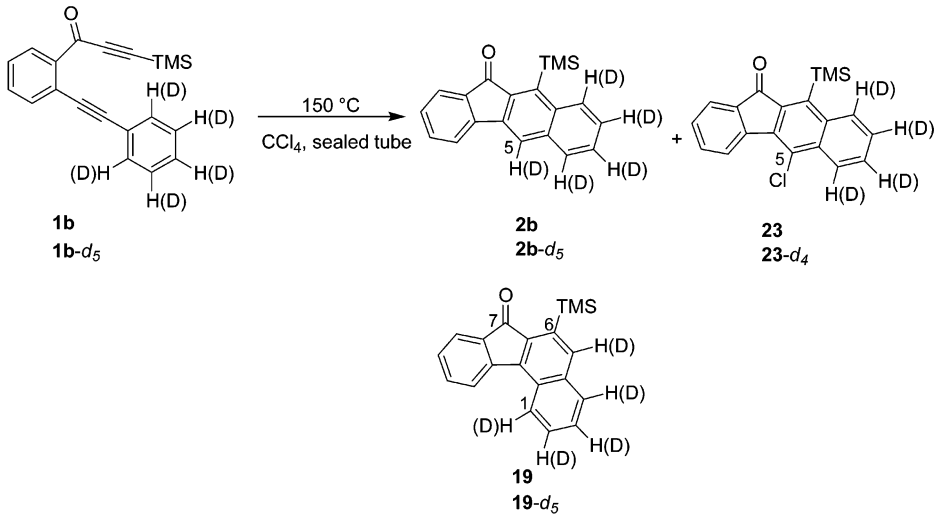

To exclude contributions to the total amount of linear benzo[*b*]fluorenone **2b** by adventitious intermolecular protonation, we repeated the experiment using deuterated **1b**-d_5 as starting material. Gratifyingly, product yields and ratios were similar to those obtained previously: a fraction containing a 10:1 mixture of benzo[*b*]-fluorenone **2b** (80% as **2b**-d_5) and benzo[*c*]fluorenone **19** in 38% combined yield was accompanied by a 44% yield of the chlorinated benzo[*c*]fluorenone **23**-d_4 (Scheme 10).

The above results seem to indicate that intermolecular radical addition of CCl_4 can compete with the intramolecular aromatization path leading to benzo[*b*]- and benzo[*c*]fluorenones. To investigate this, we studied the radical addition process computationally in the cases of the simpler intermediates **4** and **14**. PCM calculations showed that the enthalpy barrier to chlorine abstraction is 5.4 kcal/mol for cyclohexatriene **4** and as low as 2.9 kcal/mol for isonaphthalene **14** (Figure 4). Gas-phase NBO charge analysis showed that in the transition states **24** and **25** total charges of respectively −0.176 and −0.208 (−0.227 and −0.283 by the PCM calculations) are transferred from the allene to the carbon tetrachloride moiety, indicating the nucleophilic character of cyclic allenes in halogen addition reactions. Due to this transfer of charge in the transition states, solvation slightly lowers the activation barriers, to 4.9 and 2.8 kcal/mol, respectively (Figure 4).

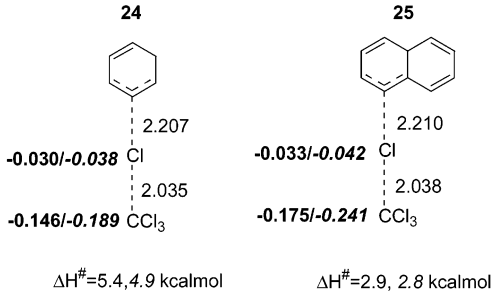

FIGURE 4. Selected parameters of transition states **24** and **25** at the B3LYP/6-311+G**//B3LYP/6-31G* level. Light face type, bond lengths; bold face type, NBO charges (chlorine and CCl_3 moieties). Left: gas-phase value. Right: PCM/toluene value. Activation enthalpies: roman type, gas-phase value; italic type, PCM/toluene value.

Interestingly, we also found that formation of a radical pair, **26**−**27**, is ca. 20 kcal/mol more favored than formation of a contact ionic pair, **28**−**29**, even when solvation effects are taken into account (Figure 5).

In conclusion, our computational results thus show, in agreement with the experimental findings, that the intermolecular and therefore entropically disfavored chlorine addition reaction can compete effectively, due to its low enthalpic barrier (2.9 kcal/mol), with the intramolecular aromatization pathway ($\Delta H = 17.9$ kcal/mol).

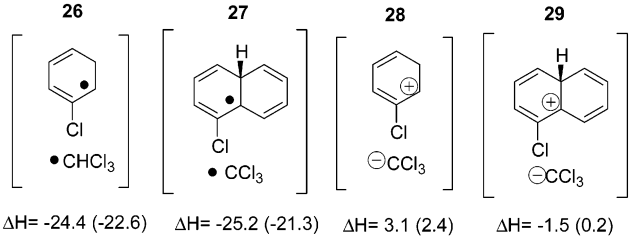

FIGURE 5. Reaction enthalpies (kcal/mol) at the B3LYP/6-311+G** level calculated for the formation of contact radical and ionic pairs from cyclic allenes and carbon tetrachloride (gas-phase values, with PCM/toluene values in parentheses).

Conclusions

To sum up, the cycloaromatization of cyclic allenes may follow both inter- and intramolecular pathways, depending on the experimental conditions. For synthetic purposes, the best procedure is to use a protic solvent to promote the ionic intermolecular route, the fastest and highest-yielding. Theoretical calculations show that benzoannulation significantly lowers the barrier to the rate-limiting [1,2] H transfer of the intramolecular route. Our calculations also predict a very low barrier for the reaction of cyclohexatrienes with carbon tetrachloride, and that cyclic allenes act as nucleophiles in this reaction.

Experimental Section

General Procedures. All reactions were carried out under argon and solvents were purified and dried following standard procedures. Deuterated compounds were characterized by mass spectrometry and TLC comparison with the corresponding protonated analogues.[5b,43]

1-[2-(*d*$_5$-Phenylethynyl)phenyl]-3-trimethylsilyl-2-propyn-1-ol (18). To a solution of **17** (1.10 g, 4.82 mmol), $PdCl_2(PPh_3)_2$ (68 mg, 0.10 mmol), and CuI (46 mg, 0.24 mmol) in THF (20 mL) and Et_3N (6 mL) was added iodobenzene-*d*$_5$ (1.01 g, 4.82 mmol) and the mixture was stirred at room temperature for 2 h. After filtration through a Celite pad, the volatiles were removed and the residue was solved in EtOAc (30 mL) and washed with aqueous HCl (5%) (2 × 30 mL) and brine (2 × 30 mL). The organic layer was dried over anhydrous Na_2SO_4 and evaporated to dryness. The crude residue was purified by column chromatography on silica gel, using hexane/EtOAc 9:1 as eluent, to yield **18** (1.13 g, 76%) as a colorless oil; ^{1}H NMR ($CDCl_3$, 250 MHz) δ 7.72 (dd, J = 7.5, 1.5 Hz, 1H), 7.56 (dd, J = 7.5, 1.3 Hz, 1H), 7.40 (td, J = 7.5, 1.5 Hz, 1H), 7.33 (td, J = 7.5, 1.3 Hz, 1H), 5.94 (d, J = 5.6 Hz, 1H), 2.66 (d, J = 5.6 Hz, 1H), 0.18 (s, 9H); ^{13}C NMR/DEPT ($CDCl_3$, 62.89 MHz) δ 141.9 (C), 132.3 (CH), 131.1 (t, J = 25 Hz, 2 × CD), 128.8 (CH), 128.2 (CH), 128.0 (t, J = 24 Hz, CD), 127.8 (t, J = 24 Hz, 2 × CD), 126.6 (CH), 122.5 (C), 121.4 (C), 104.4 (C), 94.9 (C), 91.3 (C), 86.5 (C), 63.5 (CH), −0.3 ($Si(CH_3)_3$); EI-MS *m*/*z* 309 (M^+, 50), 294 (72), 220 (64), 73 (100).

1-[2-(*d*$_5$-Phenylethynyl)phenyl]-3-trimethylsilyl-2-propyn-1-one (1b-*d*$_5$). To a solution of **18** (190 mg, 0.61 mmol) in CH_2Cl_2 (5 mL) was added small portions of activated MnO_2 until disappearance of the starting material (TLC monitoring). After filtration through a short pad of silica, the solvent was removed in a vacuum to afford **1b**-*d*$_5$ (187 mg, 99%) as a pale yellow oil in high purity (column chromatography of **1b**-*d*$_5$ should be avoided due to the instability of the trimethylsilyl ethynyl ketone in silica). ^{1}H NMR ($CDCl_3$, 250 MHz) δ 8.16−8.11 (m, 1H), 7.64 (d, J = 7.6 Hz, 1H), 7.53 (td, J = 7.6, 1.6 Hz, 1H), 7.44 (td, J = 7.6, 1.6 Hz, 1H), 0.25 (s, 9H); EI-MS *m*/*z* 307 (M^+, 100), 292 (97), 264 (39), 73 (18).

1-[2-(*d*$_5$-Phenylethynyl)phenyl]-2-propyn-1-one (1a-*d*$_5$). To a solution of **1b**-*d*$_5$ (230 mg, 0.75 mmol) in MeOH (8 mL) was added an aqueous solution of Borax (5 mL, 0.01 M) and the mixture was stirred for 2 h. After removing the volatiles the resulting residue was solved in EtOAc (20 mL) and washed with brine (3 × 20 mL). The organic layer was dried over anhydrous Na_2SO_4 and evaporated to dryness. The crude residue was purified by column chromatography on silica gel, using hexane/EtOAc 9:1 as eluent, to yield **1a**-*d*$_5$ (150 mg, 85%) as a colorless oil. **1a**-*d*$_5$ proved to be rather unstable both neat and in solution but it could be stored at −30 °C for several days. ^{1}H NMR ($CDCl_3$, 250 MHz) δ 8.19 (dd, J = 7.8, 1.5 Hz, 1H), 7.69−7.65 (m, 1H), 7.57 (td, J = 7.6, 1.5 Hz, 1H), 7.49−7.42 (m, 1H), 3.44 (s, 1H); EI-MS *m*/*z* 235 (M^+, 100), 207 (62), 204 (19).

General Procedure for Thermal Cyclizations. A solution of the ynone in dried and degassed solvent (concentration from 25 to 130 mM) was placed in a sealed tube and heated overnight at 150 °C in a silicon oil bath. After evaporation of the solvent, the crude material was purified by column chromatography on silica gel, using hexane/EtOAc as eluent.

Thermal Cyclization of 1a-*d*$_5$. A solution of **1a**-*d*$_5$ (70 mg, 0.30 mmol, 30 mM) in toluene (9 mL) and CH_3OH (1 mL) was heated under the general conditions. After column chromatography on silica gel, using hexane/EtOAc 9:1 as eluent, benzo[*b*]fluorenone **2a**-*d*$_4$ (50 mg, 72%) was isolated as a yellow solid; ^{1}H NMR ($CDCl_3$, 250 MHz) δ 8.17 (s, 1H), 7.87 (s, 1H), 7.75 (d, J = 7.2 Hz, 1H), 7.71 (d, J = 7.6 Hz, 1H), 7.56 (t, J = 7.6 Hz, 1H), 7.34 (t, J = 7.2 Hz, 1H); EI-MS *m*/*z* 234 (M^+, 100), 206 (28). Similarly, when the reaction was carried out with toluene and CH_3OD as solvents, benzo[*b*]fluorenone **2a**-*d*$_5$ (70%) was obtained; ^{1}H NMR ($CDCl_3$, 250 MHz) δ 8.17 (s, 1H), 7.75 (d, J = 7.2 Hz, 1H), 7.71 (d, J = 7.6 Hz, 1H), 7.56 (t, J = 7.6 Hz, 1H), 7.34 (t, J = 7.2 Hz, 1H); EI-MS *m*/*z* 235 (M^+, 100), 207 (27). Finally, when the reaction was carried out with benzene as solvent, a 50% yield of benzo[*b*]fluorenone **2a** was obtained, being 60% of the material **2a**-*d*$_5$ and the remaining 40% **2a**-*d*$_4$ as shown by integration of the singlet at 7.87 ppm of ^{1}H NMR of the purified product.

Thermal Cyclization of 1b-*d*$_5$ in Benzene. A solution of **1b**-*d*$_5$ (120 mg, 0.39 mmol, 65 mM) in freshly distilled benzene (6 mL) was heated under the general conditions. After evaporation of the solvent, the residue was solved in THF (6 mL) and treated with TBAF (1.00 mL, 1 M in THF). After being stirred for 2 min at room temperature, the reaction mixture was diluted with EtOAc (30 mL) and washed with brine (3 × 30 mL). The organic layer was dried over anhydrous Na_2SO_4 and evaporated to dryness. The crude residue was purified by column chromatography on silica gel, using hexane/EtOAc 9.5:0.5 as eluent, to yield benzo[*c*]fluorenone **19**-*d*$_5$ (28 mg, 23%, R_f 0.50), with 60% deuterium incorporation at position 1, as an orange solid and benzo[*b*]fluorenone **2a** (54 mg, 59%, R_f 0.25), with 70% deuterium incorporation at position 5. Compound **19**-*d*$_5$: ^{1}H NMR ($CDCl_3$, 250 MHz) δ 8.51 (s, 0.4 × 1H), 8.04 (d, J = 7.6 Hz, 1H), 7.66 (d, J = 7.6 Hz, 1H), 7.56−7.48 (m, 1H), 7.34−7.27 (m, 1H), 0.45 (s, 9H).

Thermal Cyclization of 1b in CCl_4. A solution of **1b** (250 mg, 0.76 mmol, 127 mM) in CCl_4 (6 mL) was heated under the general conditions. After column chromatography on silica gel, using hexane/EtOAc 9.25:0.25 as eluent, three products were isolated: chlorinated benzo[*b*]fluorenone **23** (83 mg, 32%, R_f 0.38) as a yellow solid and fluorenones **2b** and **19** as an inseparable mixture (94 mg, 41%, R_f 0.31) in a 6.5:1 ratio. Benzo[*b*]fluorenone **23**: mp 169−171 °C (EtOAc−hexane); ^{1}H NMR ($CDCl_3$, 250 MHz) δ 8.49 (d, J = 7.8 Hz, 1H), 8.41 (d, J = 8.5 Hz, 1H), 8.39 (dd, J = 8.0, 1.5 Hz, 1H), 7.76 (d, J = 7.6 Hz, 1H), 7.69−7.57 (m, 2H), 7.56−7.48 (m, 1H), 7.40 (t, J = 7.6 Hz, 1H), 0.58 (s, 9H); ^{13}C NMR/DEPT ($CDCl_3$, 62.89 MHz) δ 193.4 (CO), 143.3 (C), 143.2 (C), 140.6 (C), 138.9 (C), 135.7 (C), 134.8 (CH), 134.5 (C), 133.6 (C), 131.5 (CH), 129.2 (CH), 128.9 (CH), 128.5 (C), 126.7 (CH), 125.2 (CH), 125.0 (CH), 123.9 (CH), 3.0 ($Si(CH_3)_3$); EI-MS *m*/*z* 338 (M^+, 4), 336 (M^+, 12), 323 (58), 321 (100), 293 (11), 291 (30); HRMS calcd for $C_{20}H_{17}OSi^{37}Cl$ 338.07077, found 338.07218; HRMS calcd

for $C_{20}H_{17}OSi^{35}Cl$ 336.07372, found 336.07386. Elemental analysis calcd (%) for $C_{20}H_{17}OSiCl$: C 71.30, H 5.09. Found: C 71.06, H 5.12.

Thermal Cyclization of 1b-d_5 in CCl_4. A solution of **1b**-d_5 (155 mg, 0.50 mmol, 100 mM) in CCl_4 (5 mL) was heated under the general conditions. After column chromatography on silica gel, using hexane/EtOAc 9.25:0.25 as eluent, three products were isolated: chlorinated benzo[*b*]fluorenone **23**-d_4 (76 mg, 44%, R_f 0.38) as a yellow solid and fluorenones **2b** (80% as **2b**-d_5) and **19** (percentage of deuteration could not be calculated due to the low intensity of ^{1}H signals) as an inseparable mixture (59 mg, 38%, R_f 0.31) in a 10:1 ratio. Benzo[*b*]fluorenone **23**-d_4: ^{1}H NMR ($CDCl_3$, 250 MHz) δ 8.49 (d, J = 7.6 Hz, 1H), 7.75 (d, J = 7.1 Hz, 1H), 7.61 (td, J = 7.6, 1.2 Hz, 1H), 7.39 (td, J = 7.1, 1.2 Hz, 1H), 0.58 (s, 9H); EI-MS m/z 342 (M^+, 18), 340 (M^+, 56), 325 (100), 327 (36).

Acknowledgment. We thank the Dirección General de Investigación for financial support under Projects PB98-0606 and BQU2002-02135, and the Centro de Supercomputación de Galicia (CESGA) for generous allocation of computational resources. D. Rodríguez also thanks the Ministerio de Educación y Ciencia for a predoctoral grant.

Supporting Information Available: Cartesian coordinates for all computed species and absolute energies and ⟨S2⟩ values. This material is available free of charge via the Internet at http://pubs.acs.org.

JO0265380